Punjab University
Journal of Mathematics (ISSN 1016-2526)
Vol. 51(10)(2019) pp. 25-43

Boundary data completion for a diffusion-reaction equation by minimizing the energy error functional and applying the conjugate gradient method

Miled EL HAJJI
ENIT-LAMSIN, BP. 37, 1002 Tunis-Belvédère, Tunis El Manar university, Tunis, Tunisia.
Email: miled.elhajji@enit.rnu.tn

Fadhel JDAY
ENIT-LAMSIN, BP. 37, 1002 Tunis-Belvédère, Tunis El Manar university, Tunis, Tunisia.
Mathematics department, Jamoum University College, Umm al-Qura University,
Mekkah , Saudi Arabia.
Email: fadheldj@yahoo.com

Received: 16 February, 2019 / Accepted: 31 May, 2019 / Published online: 01 September, 2019

Abstract. In this paper, a boundary data completion problem for a diffusion-reaction partial differential equations (PDEs) was considered in a 2D domain. In a first step, the classical KMF (Kozlov, Maz'ya, Fomin) algorithm was used with spectral element method to find an approximate solution to that problem. In a second step, an alternative way was proposed by using conjugate gradient method where a symmetric positive definite operator was designed. Obtained results are illustrated by some numerical tests by using Matlab software.

AMS (MOS) Subject Classification Codes: 12A34; 56B78
Key Words: Diffusion-Reaction equation; Inverse problem; Data completion; Cauchy problem; Conjugate gradient method; KMF algorithm; Spectral element method.

1. INTRODUCTION

Large engineering applications such as heat conduction, some chemical reaction etc. are modelled by diffusion-reaction equations. Micro- and mini-channels, whose hydraulic diameter varies from a few micrometers to several millimetres, are increasingly used in many applications [15, 16, 17]. Condensation in these channels is used in different applications, in particular, the cooling of electronic components and the air conditioning in the automobile. The study of local heat transfer represent a real scientific key by considering its effect on the lifetime and performance of energy systems such as fuel cells and miniature coolers. In this paper, suppose that our domain is a channel filled up by a fluid and suppose that on some part of the boundary (input), measurements can be done for both the temperature and flux, however, on an other some part of the boundary (output), we suppose that

we can't do this due to physical difficulties or inaccessibility geometric. Thus, the aim is to reconstruct the temperature and the flux in an infinite length channel. We suppose that the temperature is invariable on the vertical direction. So we are dealing with a 2D-problem. This phenomena can occur in several engineering processes.
Our aim is then to reconstruct the missing data on some part of the boundary (the output: where the knowledge of the temperature at the output is necessary for ensuring the safety of the material) using the over available data on the accessible part of the boundary (input). Such problem is known as a Cauchy problem, called also data completion problem. It is difficult to resolve this kind of problems using direct method because of its ill-posedness in the sense of Hadamard [8, 9]. The existence of the solution is assured when the over determined data at the input are compatible [10] and the problem admits then at most one solution [6]. Several iterative methods having the advantage to allow the physical constraint were proposed to resolve this problem [1, 2, 3, 4, 5, 13].

In the present work, a data completion problem for a diffusion-reaction partial differential equations (PDEs) was considered in a 2D domain. In a first step, the classical KMF (Kozlov, Maz'ya, Fomin) algorithm [13] is used to find an approximate solution to that problem. In a second step, we use an alternative way by using conjugate gradient method where a symmetric positive definite operator A was designed. Obtained results are confirmed by some numerical tests under Matlab software.

2. Direct problem

Let Ω be an open bounded set in $\mathbb{R}^2$, with a smooth boundary $\partial\Omega$. We consider a partition of this boundary $\partial\Omega = \Sigma \cup \Gamma$ where $\Sigma \cap \Gamma = \emptyset$, $\text{mes}(\Sigma) \neq 0$ and $\text{mes}(\Gamma) \neq 0$. The domain Ω represents a channel filled up by a moving fluid, Σ is a fixed wall and Γ is the input and output of the channel. Γ is taken to be straight and orthogonal to the axis of the outlet (Figure 1).

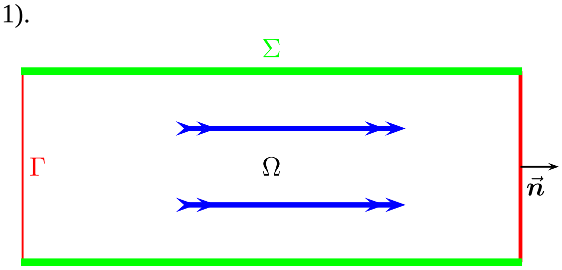

FIGURE 1. The domain Ω represents the geometry of the considered channel filled up by a moving fluid. All vertices belongs to Σ.

We are looking for finding a function u solution of the well-posed problem defined as follows:

$$\begin{cases} -\nabla.(\mu\nabla u) + \sigma u = f & \text{in} \quad \Omega \\ u = g & \text{on} \quad \Sigma \\ \mu\dfrac{\partial u}{\partial \boldsymbol{n}} = h & \text{on} \quad \Gamma \end{cases} \tag{1}$$

Where f is the source function, μ is the diffusivity constant and σ is the reaction constant. μ and σ assumed to be positive. $\vec{\boldsymbol{n}}$ is the outward-pointing normal vector. This direct problem is well-posed, it has a unique solution until $f \in L^2(\Omega)$ and it can be solved by direct method.

In order to outline the spectral element method, we first start with the variational formulation of the direct problem (1). The solution u is searched in U such that :

$$a(u,v) = l(v), \qquad \forall v \in V \tag{2}$$

where the solution space U and the test function space V are given by

$$U = \{u \in H^1(\Omega) : \ u = g \ \text{ on } \ \Sigma\}, \quad V = \{v \in H^1(\Omega) : \ v = 0 \ \text{ on } \ \Sigma\}$$

The bilinear form is

$$a(u,v) \ \ = \int_\Omega \Big(\mu \nabla u . \nabla v \ + \sigma u v\Big)\, dx,$$

and the linear form is

$$l(v) \ \ = \ \ \int_\Omega f v \ dx \ + \int_\Gamma h v \ ds.$$

Denote by N the degree of interpolation and x_i and $y_i,\ i = 1, \cdots, N+1$ are the associated nodes, known as the Gauss-Lobatto Legendre points, which are the zeros of $(1-x^2)L'_N(x)$ and $(1-y^2)L'_N(y)$, respectively.
Weights for Legendre-Gauss-Lobatto numerical integration are given by:

$$w_i = \frac{2}{N(N+1)}\frac{1}{L_N^2(x_i)}, i = 1, \cdots, N+1$$

Denote by $u_{ij} = u(x_i, y_j)$, and $f_{ij} = f(x_i, y_j)$, for $i, j = 1, \cdots, N+1$. Then u is expanded in terms of the Lagrange interpolants based on the Legendre-Gauss-Lobatto points

$$u_N(x,y) = \sum_{i,j=1}^{N+1} u_{ij} h_i(x) h_j(y)$$

where h_i are the Lagrange interpolants.

The Galerkin approximation is to solve the discrete weak problem: Find $u_N \in \mathcal{U}^N$ such that

$$a_N(u_N, v_N) := D_N(u_N, v_N) + R_N(u_N, v_N) = l_N(v_N)$$

where the forms $D_N(u_N, v_N) = (\mu \nabla u_N, \nabla v_N)_N$, and $R_N(u_N, v_N) = (\sigma\, u_N, v_N)_N$ corresponding to the diffusion and the linear reaction parts of the problem, respectively. The discrete inner product $(.,.)_N$ is defined by

$$(\varphi, \psi)_N = \sum_{m,n=1}^{N+1} w_m w_n \varphi(x_m, y_n) \psi(x_m, y_n).$$

In the rest of the paper, for simplicity and without loss of generality, we will take $\mu = \sigma = 1$.

3. INVERSE PROBLEM

Consider a partition of the part of the boundary $\Gamma = \Gamma_m \cup \Gamma_u$ where $\Gamma_m \cap \Gamma_u = \emptyset$, $\text{mes}(\Gamma_m) \neq 0$ and $\text{mes}(\Gamma_u) \neq 0$. As the domain Ω represents a channel filled up by a moving fluid, Σ is a fixed wall, Γ_m and Γ_u is the input and output of the channel, respectively which are taken to be straight and orthogonal to the axis of the outlet (Figure 2).

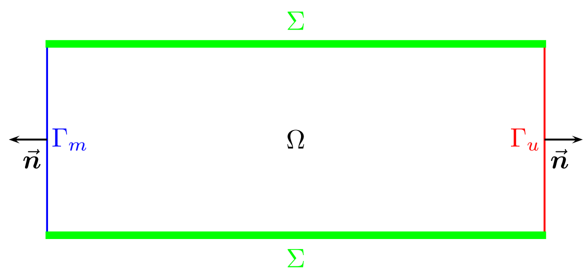

FIGURE 2. The domain Ω represents a channel filled up by a moving fluid. Σ is a fixed wall, Γ_m is the input of the channel and Γ is the output of the channel. Γ_m and Γ_u are taken to be straight and orthogonal to the axis of the outlet. $\vec{\boldsymbol{n}}$ is the outward-pointing normal vector. Note that all vertices belongs to Σ.

Suppose that we have measurements of Dirichlet (T) and Neumann boundary (Φ) conditions on the input of the channel (Γ_m) and try to recover the missing data on the output of the channel (Γ_u).

For $(f, g, \Phi, T) \in L^2(\Omega) \times H^{\frac{1}{2}}(\Sigma) \times (H^{\frac{1}{2}}(\Gamma_m))' \times H^{\frac{1}{2}}(\Gamma_m)$, the inverse problem is given by :

$$\left\{ \begin{array}{rcll} -\Delta u + u & = & f & \text{in} \quad \Omega \\ u & = & g & \text{on} \quad \Sigma \\ \dfrac{\partial u}{\partial \boldsymbol{n}} & = & \Phi & \text{on} \quad \Gamma_m \\ u & = & T & \text{on} \quad \Gamma_m \end{array} \right. \tag{3}$$

Assuming that the data (Φ, T) are compatible, i.e. this pair correspond exactly to the trace and the normal trace of the same function u that will be extended by a couple (φ, t) on Γ_u which complete the problem (3) to

$$\left\{ \begin{array}{rll} -\Delta u + u = f & \text{in} & \Omega \\ u = g & \text{on} & \Sigma \\ \dfrac{\partial u}{\partial \boldsymbol{n}} = \Phi, \ u = T & \text{on} & \Gamma_m \\ \dfrac{\partial u}{\partial \boldsymbol{n}} = \varphi, \quad u = t & \text{on} & \Gamma_u \end{array} \right. \tag{4}$$

4. The classical KMF algorithm

Many performing numerical methods have been developed to overcome the ill-posed nature of this kind of problem. In this paper, we revisit the classical KMF (Kozlov, Maz'ya, Fomin) algorithm [13] (some applications in [7, 11, 14, 18]), known as an alternating method by solving alternately two direct problems in order to approximate the missing data on the boundary. The KMF algorithm used the following steps: Let $\tau_0 \in H^{\frac{1}{2}}(\Gamma_u)$ as an initialisation for the Dirichlet boundary condition on Γ_u.

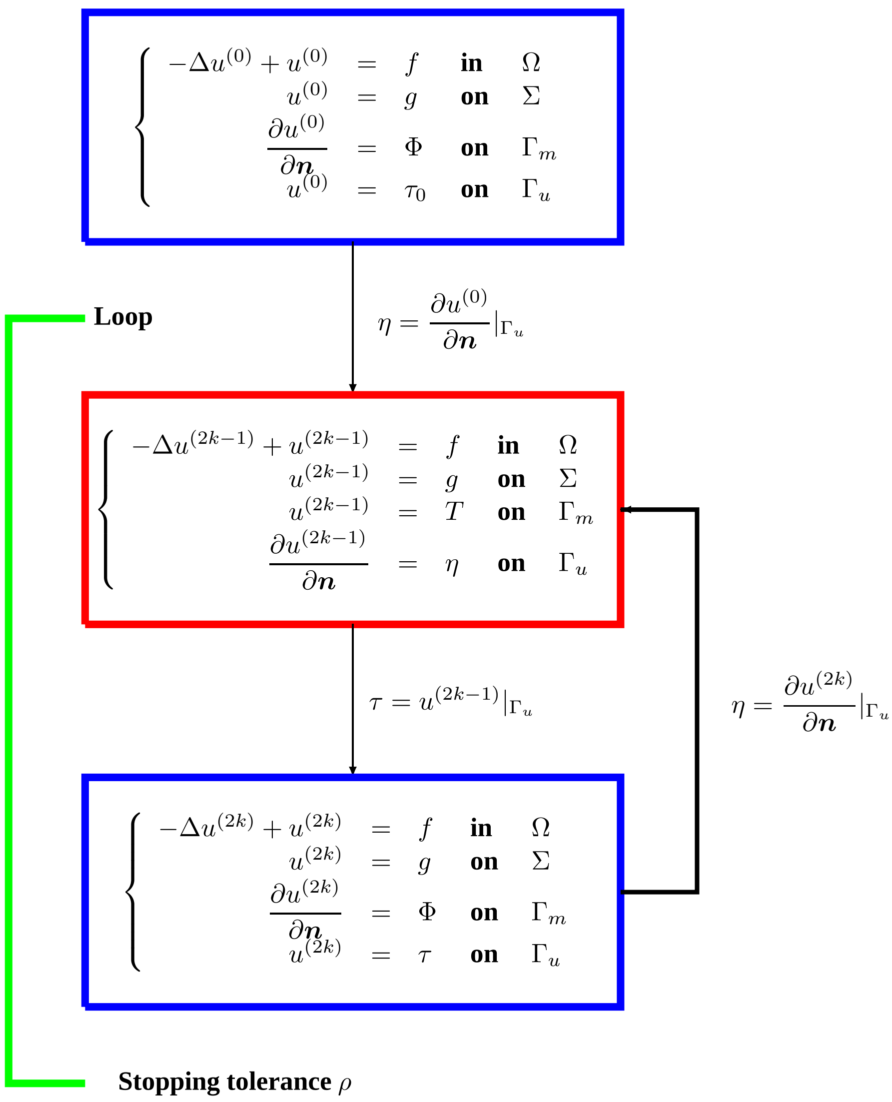

FIGURE 3. The classical KMF algorithm.

In many applications the error cannot be evaluated since the analytical solution is not known and then a stopping tolerance is imposed such that

$$\|u^{(n+1)} - u^{(n)}\|_{L^2(\Gamma_u)} < \rho$$

where ρ is a positive small enough constant.
If (Φ, T) are compatible then $u^{2k-1} = u^{2k}$ when $(\eta, \tau) = (\varphi, t)$.
The cost function is a norm for controlling $u^{(2k-1)} - u^{(2k)}$ on the hole domain Ω.

5. Minimum of an energy functional

To solve the problem (4), (φ, t) will be characterized as the minimum of an energy functional [2, 3, 5, 7, 12, 14]. The approach is to consider, for a given pair (η, τ), two mixed problems where their solutions are denoted by u_1 and u_2 and satisfying:

$$\left\{\begin{array}{rcll} -\Delta u_1 + u_1 &=& f & \text{in} \quad \Omega \\ u_1 &=& g & \text{on} \quad \Sigma \\ u_1 &=& T & \text{on} \quad \Gamma_m \\ \dfrac{\partial u_1}{\partial \boldsymbol{n}} &=& \eta & \text{on} \quad \Gamma_u \end{array}\right. \qquad (5) \qquad \left\{\begin{array}{rcll} -\Delta u_2 + u_2 &=& f & \text{in} \quad \Omega \\ u_2 &=& g & \text{on} \quad \Sigma \\ \dfrac{\partial u_2}{\partial \boldsymbol{n}} &=& \Phi & \text{on} \quad \Gamma_m \\ u_2 &=& \tau & \text{on} \quad \Gamma_u \end{array}\right. \qquad (6)$$

and to construct an error functional based on the pair (η, τ) through the comparison of the fields u_1 and u_2. These fields coincide only if the couple (η, τ) coincide with the real data (φ, t) on the unmeasured boundary Γ_u. That's why we chosed to solve this Cauchy problem as follows:

$$\left\{\begin{array}{l} (\varphi, t) = \text{arg}\min\limits_{\eta,\tau} \; E(\eta, \tau) \\ E(\eta, \tau) := \|u_1 - u_2\|^2_{H^1(\Omega)} = \displaystyle\int_\Omega (\nabla u_1 - \nabla u_2)^2 + \int_\Omega (u_1 - u_2)^2 \\ u_1, u_2 \quad \text{are solution of systems } (5) and (6), \text{ respectively} \end{array}\right. \qquad (7)$$

Note that $E(\eta, \tau)$ is a convex quadratic positive functional attenuating its minimum at $u_1 = u_2$.
Now, since u_1 and u_2 are solutions of (5) and (6), it is easy to derive a more simple expression of the error functional:

$$\begin{array}{rcl} E(\eta, \tau) &=& -\displaystyle\int_\Omega \Delta(u_1 - u_2)(u_1 - u_2) + \int_{\Gamma_u} (\eta - \frac{\partial u_2}{\partial \boldsymbol{n}})(u_1 - \tau) \\ &+& \displaystyle\int_{\Gamma_m} (\frac{\partial u_1}{\partial \boldsymbol{n}} - \Phi)(T - u_2) + \int_\Omega (u_1 - u_2)^2 \\ &=& \displaystyle\int_{\Gamma_u} (\eta - \frac{\partial u_2}{\partial \boldsymbol{n}})(u_1 - \tau) + \int_{\Gamma_m} (\frac{\partial u_1}{\partial \boldsymbol{n}} - \Phi)(T - u_2) \end{array}$$

The gradient of the error functional is then given by: For a pair (η, τ)

$$\begin{array}{l} \dfrac{\partial E(\eta, \tau)}{\partial \eta}\psi = \displaystyle\int_{\Gamma_u} [u_1 - \tau]\psi + \int_{\Gamma_m} \frac{\partial w_1}{\partial \boldsymbol{n}}[T - u_2] \\ \dfrac{\partial E(\eta, \tau)}{\partial \tau}h = \displaystyle\int_{\Gamma_u} [\frac{\partial u_2}{\partial \boldsymbol{n}} - \eta]h + \int_{\Gamma_m} [\Phi - \frac{\partial u_1}{\partial \boldsymbol{n}}]w_2 \end{array} \qquad (8)$$

for all $(h, \psi) \in H_{00}^{1/2}(\Gamma_u) \times H_{00}^{-1/2}(\Gamma_u)$, and where w_1 and w_2 solve

$$\begin{cases} -\Delta w_1 + w_1 &= 0 \quad \text{on} \quad \Omega \\ w_1 &= 0 \quad \text{on} \quad \Sigma \\ w_1 &= 0 \quad \text{on} \quad \Gamma_m \\ \dfrac{\partial w_1}{\partial \boldsymbol{n}} &= \psi \quad \text{on} \quad \Gamma_u \end{cases} \quad (9) \qquad \begin{cases} -\Delta w_2 + w_2 &= 0 \quad \text{in} \quad \Omega \\ w_2 &= 0 \quad \text{on} \quad \Sigma \\ \dfrac{\partial w_2}{\partial \boldsymbol{n}} &= 0 \quad \text{on} \quad \Gamma_m \\ w_2 &= h \quad \text{on} \quad \Gamma_u \end{cases} \quad (10)$$

Problems (9) and (10) depend on the directions ψ and h.

The components of the gradient can be given in a more simple form by applying the adjoint state method, that the gradient will be evaluated in any direction using only the determination of two adjoint fields v_1 and v_2.

Proposition 1.

$$\frac{\partial E(\eta,\tau)}{\partial \eta}\psi = -2\int_{\Gamma_u} v_1\psi \quad \textit{and} \qquad \frac{\partial E(\eta,\tau)}{\partial \tau}h = -2\int_{\Gamma_u} \frac{\partial v_2}{\partial \boldsymbol{n}}h,$$

where v_1 *and* v_2 *solve*

$$\begin{cases} -\Delta v_1 + v_1 &= 0 \quad \textit{in} \quad \Omega \\ v_1 &= 0 \quad \textit{on} \quad \Sigma \\ v_1 &= 0 \quad \textit{on} \quad \Gamma_m \\ \dfrac{\partial v_1}{\partial \boldsymbol{n}} &= \dfrac{\partial u_2}{\partial \boldsymbol{n}} - \eta \quad \textit{on} \quad \Gamma_u \end{cases} \quad (11) \qquad \begin{cases} -\Delta v_2 + v_2 &= 0 \quad \textit{in} \quad \Omega \\ v_2 &= 0 \quad \textit{on} \quad \Sigma \\ \dfrac{\partial v_2}{\partial \boldsymbol{n}} &= 0 \quad \textit{on} \quad \Gamma_m \\ v_2 &= u_1 - \tau \quad \textit{on} \quad \Gamma_u \end{cases} \quad (12)$$

6. Conjugate gradient algorithm

In numerical analysis, the conjugate gradient method is an algorithm for solving systems of linear equations whose matrix is positive symmetric definite. In numerical optimization, the non-linear conjugate gradient method generalizes the conjugate gradient method to non-linear optimization. For a quadratic function $\Psi(x)$:

$$\Psi(x) = \frac{1}{2}x^tAx - b^tx.$$

The minimum of Ψ is obtained when the gradient $\nabla\Psi(x) = Ax - b$ is zero.

The idea is mainly based on subdividing the state fields into subsystems as the following :

$$u_1 = u_1^0 + u_1^*, \quad u_2 = u_2^0 + u_2^*$$

where u_1^*, u_2^*, u_1^0 and u_2^0 are solutions of the following systems

$$\begin{cases} -\Delta u_1^* + u_1^* &= 0 \quad \text{in} \quad \Omega \\ u_1^* &= 0 \quad \text{on} \quad \Sigma \\ u_1^* &= 0 \quad \text{on} \quad \Gamma_m \\ \dfrac{\partial u_1^*}{\partial \boldsymbol{n}} &= \eta \quad \text{on} \quad \Gamma_u \end{cases} \quad (13) \qquad \begin{cases} -\Delta u_2^* + u_2^* &= 0 \quad \text{in} \quad \Omega \\ u_2^* &= 0 \quad \text{on} \quad \Sigma \\ \dfrac{\partial u_2^*}{\partial \boldsymbol{n}} &= 0 \quad \text{on} \quad \Gamma_m \\ u_2^* &= \tau \quad \text{on} \quad \Gamma_u \end{cases} \quad (14)$$

$$\begin{cases} -\Delta u_1^0 + u_1^0 = f & \text{in} \quad \Omega \\ u_1^0 = g & \text{on} \quad \Sigma \\ u_1^0 = T & \text{on} \quad \Gamma_m \\ \dfrac{\partial u_1^0}{\partial \boldsymbol{n}} = 0 & \text{on} \quad \Gamma_u \end{cases} \quad (15) \qquad \begin{cases} -\Delta u_2^0 + u_2^0 = f & \text{in} \quad \Omega \\ u_2^0 = g & \text{on} \quad \Sigma \\ \dfrac{\partial u_2^0}{\partial \boldsymbol{n}} = \Phi & \text{on} \quad \Gamma_m \\ u_2^0 = 0 & \text{on} \quad \Gamma_u \end{cases} \quad (16)$$

Same, we sub-divise the adjoint fields into the following subsystems :

$$v_1 = v_1^0 + v_1^*, \quad v_2 = v_2^0 + v_2^*$$

where v_1^*, v_2^*, v_1^0 and v_2^0 in $H^1(\Omega)$ are solutions of

$$\begin{cases} -\Delta v_1^* + v_1^* = 0 & \text{in} \quad \Omega \\ v_1^* = 0 & \text{on} \quad \Sigma \\ v_1^* = 0 & \text{on} \quad \Gamma_m \\ \dfrac{\partial v_1^*}{\partial \boldsymbol{n}} = \dfrac{\partial u_2^*}{\partial \boldsymbol{n}} - \eta & \text{on} \quad \Gamma_u \end{cases} \quad (17) \qquad \begin{cases} -\Delta v_2^* + v_2^* = 0 & \text{in} \quad \Omega \\ v_2^* = 0 & \text{on} \quad \Sigma \\ \dfrac{\partial v_2^*}{\partial \boldsymbol{n}} = 0 & \text{on} \quad \Gamma_m \\ v_2^* = u_1^* - \tau & \text{on} \quad \Gamma_u \end{cases} \quad (18)$$

$$\begin{cases} -\Delta v_1^0 + v_1^0 = 0 & \text{in} \quad \Omega \\ v_1^0 = 0 & \text{on} \quad \Sigma \\ v_1^0 = 0 & \text{on} \quad \Gamma_m \\ \dfrac{\partial v_1^0}{\partial \boldsymbol{n}} = \dfrac{\partial u_2^0}{\partial \boldsymbol{n}} & \text{on} \quad \Gamma_u \end{cases} \quad (19) \qquad \begin{cases} -\Delta v_2^0 + v_2^0 = 0 & \text{in} \quad \Omega \\ v_2^0 = 0 & \text{on} \quad \Sigma \\ \dfrac{\partial v_2^0}{\partial \boldsymbol{n}} = 0 & \text{on} \quad \Gamma_m \\ v_2^0 = u_1^0 & \text{on} \quad \Gamma_u \end{cases} \quad (20)$$

Consider the linear operator A defined by

$$\forall (\eta, \tau) \in H_{00}^{-\frac{1}{2}}(\Gamma_u) \times H_{00}^{\frac{1}{2}}(\Gamma_u), \quad A(\eta, \tau)^T = -\Big(v_1^*(\eta, \tau)|_{\Gamma_u}, \ \frac{\partial v_2^*(\eta, \tau)}{\partial \boldsymbol{n}}|_{\Gamma_u} \Big)^T .$$

Proposition 2. (1) *The energy-like functional is expressed as*

$$\forall (\eta, \tau) \in H_{00}^{-\frac{1}{2}}(\Gamma_u) \times H_{00}^{\frac{1}{2}}(\Gamma_u), \quad E(\eta, \tau) = (\eta, \tau) A (\eta, \tau)^T - 2b(\eta, \tau)^T + C_0$$

with $b = \Big(v_1^0|_{\Gamma_u}, \ \dfrac{\partial v_2^0}{\partial \boldsymbol{n}}|_{\Gamma_u} \Big)$ *, and* C_0 *be a constant independent of* (η, τ).

(2) A *is a symmetric positive-definite operator*

The Conjugate Gradient (CG) Algorithm

(1) Resolve systems (15)-(16)-(19)-(20) for one time.
(2) Choose an initial guess $x_0 = (\eta_0, \tau_0)$. Resolve systems (13)-(14)-(17)-(18) and compute $r_0 = Ax_0 - b$.
(3) Set $p_0 = -r_0$.
(4) For $k = 0, 1, 2, ...$, compute

$$\begin{aligned} \alpha_k &= \frac{r_k^T r_k}{p_k^T A p_k} \\ x_{k+1} &= x_k + \alpha_k p_k \\ r_{k+1} &= r_k + \alpha_k A p_k \\ \beta_{k+1} &= \frac{r_{k+1}^T r_{k+1}}{r_k^T r_k} \\ p_{k+1} &= -r_{k+1} + \beta_{k+1} p_k \end{aligned}$$

(5) Resolve systems (13)-(14)-(17)-(18) and compute Ap_{k+1}.
until convergence stopping criterion is satisfied ($r_k \approx 0$).

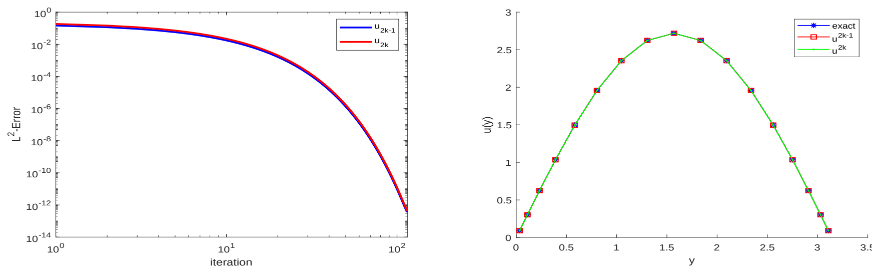

(A) loglog plot of the L^2-relative errors on the missed boundary of the reconstructed solutions.

(B) Solution on the missed boundary.

FIGURE 4. This numerical experiment is performed on a rectangular domain $[0, 1] \times [0, \pi]$. The number of nodes by each side is $N = 18$. Initial condition τ_0 is chosen randomly. As we can see on the figure, the KMF algorithm converges exponentially for only 115 iterations and with an error of order 10^{-13}.

7. NUMERICAL RESULTS

In this section we present some numerical tests which are in accordance with the theoretical given results. The implementation of this data recover method was carried out using the spectral element method (SEM). All our numerical tests are validated on a rectangular domain $[x_a, x_b] \times [y_a, y_b]$ for $\mu = \sigma = 1$.
Recall that our idea consists in a minimization of an energy error functional using conjugate gradient method. It requires the resolution of four direct systems (15)-(16)-(19)-(20) for one time and four direct systems (13)-(14)-(17)-(18) for each iteration however KMF's algorithm resolve only two direct systems. In order to prove its performance, we apply the KMF-algorithm with E as a convergence criterion. It is seen that the number of iterations of the KMF algorithm is clearly smaller that the number of iteration needed by our method. We provide the behaviour of the error between the recovered and exact data on the unmeasured boundary of the domain (output).
In our first numerical test, we used the harmonic function $u(x, y) = e^x \sin(y)$ on the rectangular domain $\Omega = [0, 1] \times [0, \pi]$ where $f(x, y) = e^x \sin(y), T(y) = e \sin(y)$ and $\Phi(y) = -e \sin(y)$. Figures 4(a) and 5(a) describe the L^2-error between exact solution and the approximated one using both KMF method and the proposed method, respectively. Figures 4(b) and 5(b) show the distribution of the reconstructed temperature and fluxes (using both KMF method and our proposed method) on the unmeasured boundary, Γ_u, as well as the exact ones. As it can be seen on all figures, the reconstructed solutions are close to the exact ones. Eighteen nodes on Γ_u and Eighteen nodes on Γ_m are sufficient to recover the

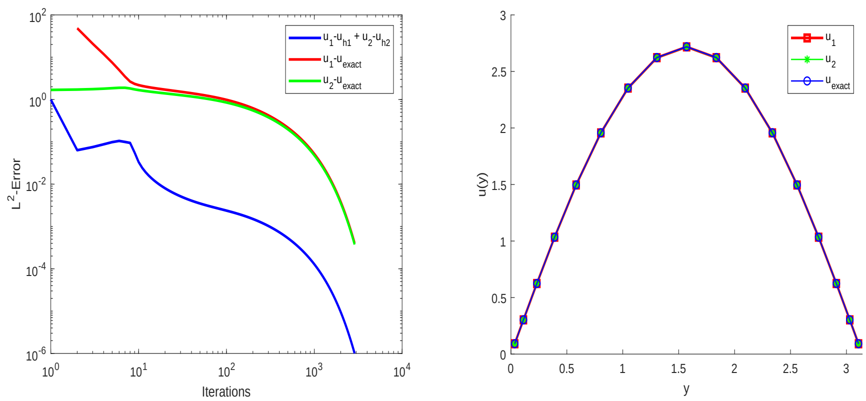

(A) loglog plot of the L^2-relative errors on the missed boundary of the reconstructed solutions.

(B) Solution on the missed boundary.

FIGURE 5. L^2-error for a randomly chosen initial condition τ_0 using the proposed Conjugate gradient method. The polynomial degree $N = 18$. The method converges exponentially for about 2800 iterations and with an error of order 10^{-4}.

trace and the normal trace with the same accuracy.
In a second numerical test, we used the function $u(x, y) = (1 + x + x^2)\sin(y)$ on the rectangular domain $\Omega = [0, 1] \times [0, 2\pi]$ where $f(x, y) = (2x + 2x^2)\sin(y), T(y) = \sin(y)$ and $\Phi(y) = -\sin(y)$. Figures 8(a) and 9(a) describe the L^2-error between exact solution and the approximated one using both KMF method and the proposed method, respectively. Figures 8(b) and 9(b) show the distribution of the reconstructed temperature and fluxes (using both KMF method and our proposed method) on the unmeasured boundary, Γ_u, as well as the exact ones. Note that the reconstructed fields are in close agreement with the exact ones. Gap between the exact and the reconstructed solution using KMF is presented in Figure 10. The gap between the exact and the reconstructed solutions u_1 and u_2 using the Conjugate gradient method is presented in Figure 12. As it can be seen on these figures, the highest values are related the unmeasured boundary Γ_u (right side).
Eighteen nodes on Γ_u and Eighteen nodes on Γ_m are enough to recover the temperature and the flux with the same accuracy.

Here, we add a numerical test for the case where $\sigma = 10$ using the KMF algorithm.

8. CONCLUSION

We proposed in this work a data completion problem for a diffusion-reaction partial differential equations (PDEs) in a 2D domain based on the minimization of an energy error

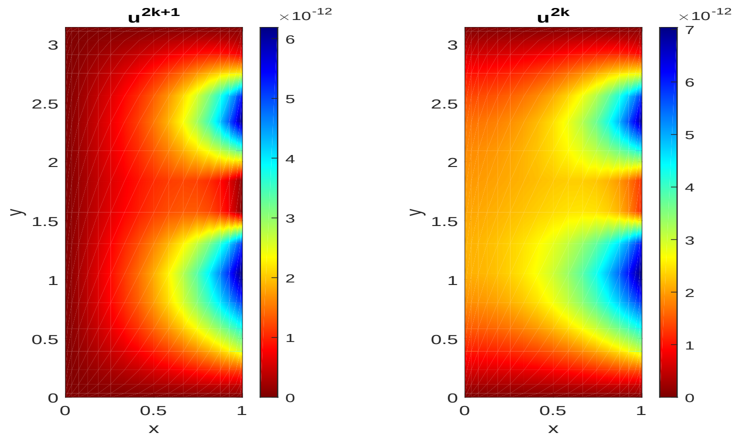

FIGURE 6. Gap between the exact and the reconstructed solution using KMF on $[0,1]\times[0,\pi]$ where the number of nodes by each side is $N = 18$. As it can be seen on the gap that highest values are related the unmeasured boundary Γ_u (right side). Highest values are about 6×10^{-12}.

functional using the conjugate gradient method. This method is undoubtedly versatile, accurate and can be developed for other operators as well as in 3D situations. The peculiarity of this method lies in the simultaneous treatment of reconstituted traces and normal traces: both are well recovered.

AUTHORS' CONTRIBUTIONS

The two authors contributed equally to the manuscript and typed, read, and approved the final manuscript.

ACKNOWLEDGEMENTS

The authors would like to thank the editor and the anonymous reviewers for their valuable comments and constructive suggestions to improve the quality of this paper.

APPENDIX A. APPENDIX

This appendix provides the mathematical proofs of Proposition 1 and Proposition 2.

A.1. **Proof of Proposition 1.**

$$\begin{aligned}
\frac{\partial E(\eta,\tau)}{\partial \eta}\psi &= 2\int_\Omega (\nabla u_1 - \nabla u_2)\nabla w_1 + 2\int_\Omega (u_1-u_2)w_1 \\
&= -2\int_\Omega (\Delta u_1 - \Delta u_2)w_1 + 2\int_{\Gamma_u} (\frac{\partial u_1}{\partial \boldsymbol{n}} - \frac{\partial u_2}{\partial \boldsymbol{n}})w_1 + 2\int_\Omega (u_1-u_2)w_1 \\
&= 2\int_{\Gamma_u} (\frac{\partial u_1}{\partial \boldsymbol{n}} - \frac{\partial u_2}{\partial \boldsymbol{n}})w_1
\end{aligned}$$

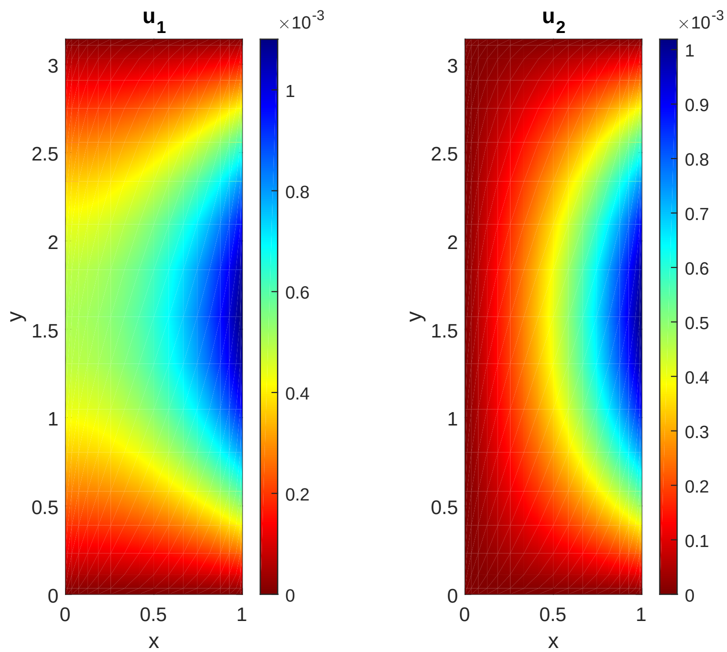

FIGURE 7. Gap between the exact and the reconstructed solutions u_1 and u_2 using the Conjugate gradient method on $[0,1]\times[0,\pi]$ where the number of nodes by each side is $N = 18$. As it can be seen on the gap that highest values are related the unmeasured boundary Γ_u (right side). Highest values are about 10^{-3}.

$$
\begin{aligned}
&= 2\int_{\Gamma_u}(\eta - \frac{\partial u_2}{\partial \boldsymbol{n}})w_1 \\
&= -2\int_{\Gamma_u}\frac{\partial v_1}{\partial \boldsymbol{n}}w_1 \\
&= -2\int_{\Omega}\nabla v_1 \nabla w_1 - 2\int_{\Omega}\Delta v_1 w_1 \\
&= -2\int_{\Omega}\nabla v_1 \nabla w_1 - 2\int_{\Omega} v_1 w_1 \\
&= 2\int_{\Omega}\Delta w_1 v_1 - 2\int_{\Gamma_u}\frac{\partial w_1}{\partial \boldsymbol{n}}v_1 - 2\int_{\Omega} w_1 v_1 \\
&= -2\int_{\Gamma_u}\frac{\partial w_1}{\partial \boldsymbol{n}}v_1 = -2\int_{\Gamma_u} v_1 \psi
\end{aligned}
$$

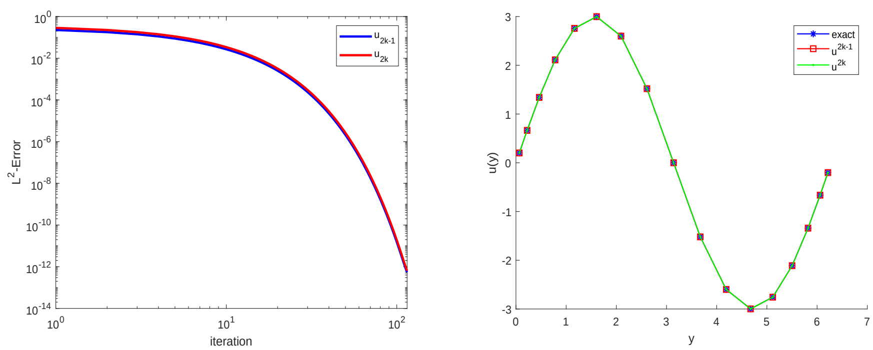

(A) loglog plot of the L^2-relative errors on the missed boundary of the reconstructed solutions.

(B) Solution on the missed boundary.

FIGURE 8. This numerical experiment is performed on a rectangular domain $[0,1]\times[0,2\pi]$. The number of nodes by each side is $N = 18$. Initial condition τ_0 is chosen randomly. As we can see on the figure, the KMF algorithm converges exponentially for only 115 iterations and with an error of order 10^{-12}.

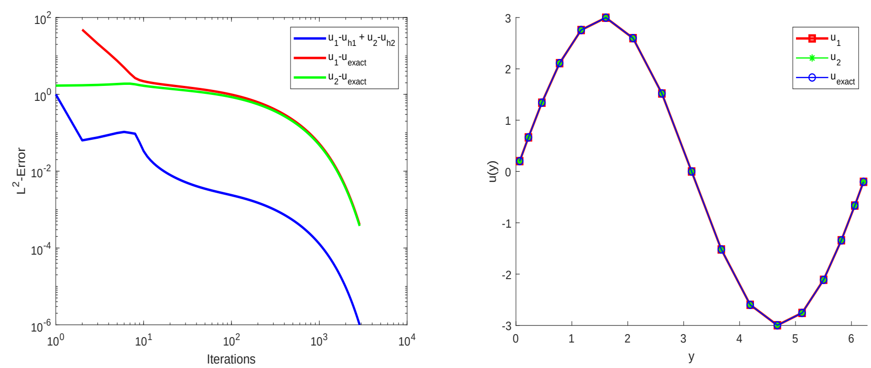

(A) loglog plot of the L^2-relative errors on the missed boundary of the reconstructed solutions.

(B) Solution on the missed boundary.

FIGURE 9. L^2-error for a randomly chosen initial condition τ_0 on a rectangular domain $[0,1]\times[0,2\pi]$. The number of nodes by each side is $N = 18$. The method converges exponentially for about 2800 iterations and with an error of order 10^{-4}.

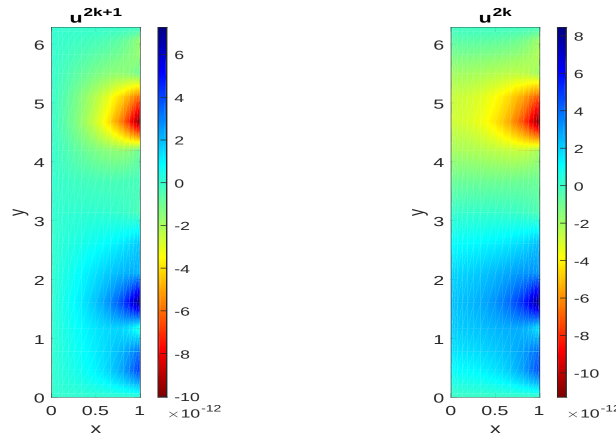

FIGURE 10. Gap between the exact and the reconstructed solution using KMF on $[0,1] \times [0,2\pi]$ where the number of nodes by each side is $N = 18$. As it can be seen on the gap that highest values are related the unmeasured boundary Γ_u (right side). Highest values are about $\pm 6 \times 10^{-12}$.

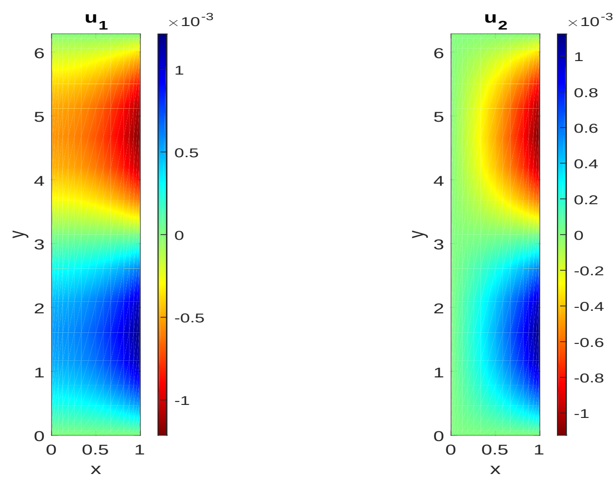

FIGURE 11. Gap between the exact and the reconstructed solutions u_1 and u_2 using the Conjugate gradient method on $[0,1] \times [0,2\pi]$ where the number of nodes by each side is $N = 18$. As it can be seen on the gap that highest values are related the unmeasured boundary Γ_u (right side). Highest values are about $\pm 10^{-3}$.

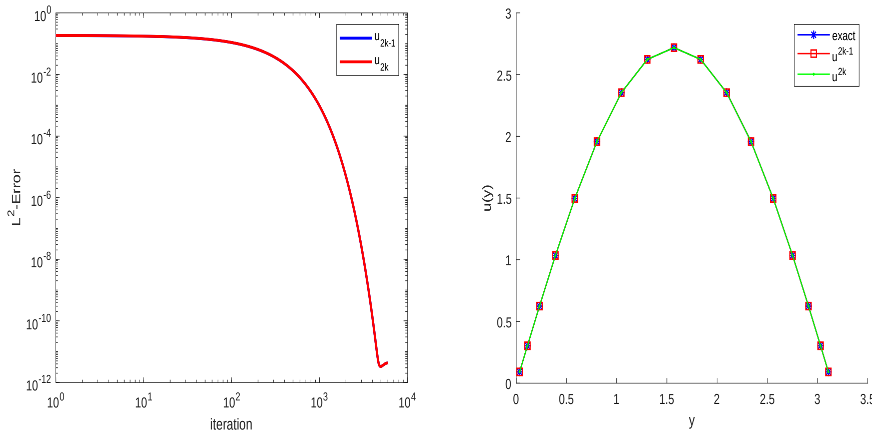

(A) loglog plot of the L^2-relative errors on the missed boundary of the reconstructed solutions.

(B) Solution on the missed boundary.

FIGURE 12. L^2-error for $u(x,y) = e^x \sin(y)$ on the rectangular domain $\Omega = [0,1] \times [0,\pi]$ where $\sigma = 10$, $f(x,y) = 10e^x \sin(y), T(y) = e\sin(y)$ and $\Phi(y) = -e\sin(y)$. The number of nodes by each side is $N = 18$. The KMF algorithm converges exponentially for about 5000 iterations and with an error of order 10^{-12}. Note that this case (large value of σ) needs more number of iterations than the case where $\sigma = 1$.

$$
\begin{aligned}
\frac{\partial E(\eta,\tau)}{\partial \tau} h &= -2\int_\Omega (\nabla u_1 - \nabla u_2)\nabla w_2 - 2\int_\Omega (u_1 - u_2) w_2 \\
&= 2\int_\Omega \Delta w_2 (u_1 - u_2) - 2\int_{\Gamma_u} \frac{\partial w_2}{\partial \boldsymbol{n}}(u_1 - u_2) - 2\int_\Omega (u_1 - u_2) w_2 \\
&= -2\int_{\Gamma_u} \frac{\partial w_2}{\partial \boldsymbol{n}}(u_1 - u_2) \\
&= -2\int_{\Gamma_u} \frac{\partial w_2}{\partial \boldsymbol{n}}(u_1 - \tau) \\
&= -2\int_{\Gamma_u} \frac{\partial w_2}{\partial \boldsymbol{n}} v_2 \\
&= -2\int_\Omega \Delta w_2 v_2 - 2\int_\Omega \nabla w_2 \nabla v_2 \\
&= -2\int_\Omega w_2 v_2 + 2\int_\Omega w_2 \Delta v_2 - 2\int_{\Gamma_u} \frac{\partial v_2}{\partial \boldsymbol{n}} w_2 \\
&= -2\int_\Omega w_2 v_2 + 2\int_\Omega w_2 v_2 - 2\int_{\Gamma_u} \frac{\partial v_2}{\partial \boldsymbol{n}} w_2 \\
&= -2\int_{\Gamma_u} \frac{\partial v_2}{\partial \boldsymbol{n}} w_2 = -2\int_{\Gamma_u} \frac{\partial v_2}{\partial \boldsymbol{n}} h
\end{aligned}
$$

A.2. **Proof of Proposition 2.**

$$
\begin{aligned}
E(\eta,\tau) &= \int_\Omega (\nabla u_1 - \nabla u_2)^2 + \int_\Omega (u_1 - u_2)^2 \\
&= -\int_\Omega (\Delta u_1 - \Delta u_2)(u_1 - u_2) + \int_{\Gamma_m \cup \Gamma_u} (\frac{\partial u_1}{\partial \boldsymbol{n}} - \frac{\partial u_2}{\partial \boldsymbol{n}})(u_1 - u_2) + \int_\Omega (u_1 - u_2)^2 \\
&= \int_{\Gamma_m} (\frac{\partial u_1}{\partial \boldsymbol{n}} - \frac{\partial u_2}{\partial \boldsymbol{n}})(u_1 - u_2) + \int_{\Gamma_u} (\frac{\partial u_1}{\partial \boldsymbol{n}} - \frac{\partial u_2}{\partial \boldsymbol{n}})(u_1 - u_2) \\
&= \int_{\Gamma_m} (\frac{\partial u_1}{\partial \boldsymbol{n}} - \Phi)(T - u_2) + \int_{\Gamma_u} (\eta - \frac{\partial u_2}{\partial \boldsymbol{n}})(u_1 - \tau) \\
&= \int_{\Gamma_m} (\frac{\partial u_1}{\partial \boldsymbol{n}} T - \Phi T + \Phi u_2 - \frac{\partial u_1}{\partial \boldsymbol{n}} u_2) + \int_{\Gamma_u} (\eta - \frac{\partial u_2}{\partial \boldsymbol{n}})(u_1 - \tau)
\end{aligned}
$$

Now, by applying Green formula to the term $\frac{\partial u_1}{\partial \boldsymbol{n}} u_2$, one obtains

$$
\begin{aligned}
\int_{\Gamma_m} \frac{\partial u_1}{\partial \boldsymbol{n}} u_2 &= \int_\Omega \Delta u_1 u_2 + \int_\Omega \nabla u_1 \nabla u_2 - \int_{\Gamma_u} \frac{\partial u_1}{\partial \boldsymbol{n}} u_2 - \int_\Sigma \frac{\partial u_1}{\partial \boldsymbol{n}} u_2 \\
&= \int_\Omega (u_1 - f) u_2 - \int_\Omega u_1 \Delta u_2 + \int_{\Gamma_m} \frac{\partial u_2}{\partial \boldsymbol{n}} u_1 + \int_{\Gamma_u} \frac{\partial u_2}{\partial \boldsymbol{n}} u_1 + \int_\Sigma \frac{\partial u_2}{\partial \boldsymbol{n}} u_1 - \int_{\Gamma_u} \eta\tau - \int_\Sigma \frac{\partial u_1}{\partial \boldsymbol{n}} g \\
&= \int_\Omega (u_1 - f) u_2 - \int_\Omega u_1 (u_2 - f) + \int_{\Gamma_m} \frac{\partial u_2}{\partial \boldsymbol{n}} u_1 + \int_{\Gamma_u} \frac{\partial u_2}{\partial \boldsymbol{n}} u_1 + \int_\Sigma \frac{\partial u_2}{\partial \boldsymbol{n}} u_1 - \int_{\Gamma_u} \eta\tau - \int_\Sigma \frac{\partial u_1}{\partial \boldsymbol{n}} g \\
&= \int_\Omega f(u_1 - u_2) + \int_{\Gamma_m} \Phi T + \int_{\Gamma_u} (\frac{\partial u_2}{\partial \boldsymbol{n}} u_1 - \eta\tau) + \int_\Sigma (\frac{\partial u_2}{\partial \boldsymbol{n}} - \frac{\partial u_1}{\partial \boldsymbol{n}}) g
\end{aligned}
$$

Thus, the energy functional becomes

$$
\begin{aligned}
E(\eta,\tau) &= \int_{\Gamma_m} (\frac{\partial u_1}{\partial \boldsymbol{n}} T - \Phi T + \Phi u_2 - \frac{\partial u_1}{\partial \boldsymbol{n}} u_2) + \int_{\Gamma_u} (\eta - \frac{\partial u_2}{\partial \boldsymbol{n}})(u_1 - \tau) \\
&= -\int_\Omega f(u_1 - u_2) + \int_\Sigma (\frac{\partial u_1}{\partial \boldsymbol{n}} - \frac{\partial u_2}{\partial \boldsymbol{n}}) g + \int_{\Gamma_m} (\frac{\partial u_1}{\partial \boldsymbol{n}} T - 2\Phi T + \Phi u_2) \\
&\quad + \int_{\Gamma_u} (\eta - \frac{\partial u_2}{\partial \boldsymbol{n}})(u_1 - \tau) + \int_{\Gamma_u} (\eta\tau - \frac{\partial u_2}{\partial \boldsymbol{n}} u_1) \\
&= -\int_\Omega f(u_1 - u_2) + \int_\Sigma (\frac{\partial u_1}{\partial \boldsymbol{n}} - \frac{\partial u_2}{\partial \boldsymbol{n}}) g + \int_{\Gamma_m} (\frac{\partial u_1}{\partial \boldsymbol{n}} u_1^0 - 2\Phi T + \frac{\partial u_2^0}{\partial \boldsymbol{n}} u_2) \\
&\quad + \int_{\Gamma_u} (\eta - \frac{\partial u_2}{\partial \boldsymbol{n}})(u_1 - \tau) + \int_{\Gamma_u} (\eta\tau - \frac{\partial u_2}{\partial \boldsymbol{n}} u_1)
\end{aligned}
$$

As before, apply Green formula to terms $\frac{\partial u_1}{\partial \boldsymbol{n}} u_1^0$ and $\frac{\partial u_2^0}{\partial \boldsymbol{n}} u_2$, one obtains

$$
\int_{\Gamma_m} \frac{\partial u_1}{\partial \boldsymbol{n}} u_1^0 = \int_\Omega f(u_1 - u_1^0) + \int_{\Gamma_m} \frac{\partial u_1^0}{\partial \boldsymbol{n}} T + \int_\Sigma (\frac{\partial u_1^0}{\partial \boldsymbol{n}} - \frac{\partial u_1}{\partial \boldsymbol{n}}) g - \int_{\Gamma_u} \eta u_1^0
$$

$$
\int_{\Gamma_m} \frac{\partial u_2^0}{\partial \boldsymbol{n}} u_2 = \int_\Omega f(u_2^0 - u_2) + \int_{\Gamma_m} \Phi u_2^0 + \int_\Sigma (\frac{\partial u_2}{\partial \boldsymbol{n}} - \frac{\partial u_2^0}{\partial \boldsymbol{n}}) g - \int_{\Gamma_u} \tau \frac{\partial u_2^0}{\partial \boldsymbol{n}}
$$

Then

$$\begin{aligned} E(\eta,\tau) &= \int_\Omega f(u_2^0-u_1^0)+\int_{\Gamma_m}(\frac{\partial u_1^0}{\partial \boldsymbol{n}}T-2\Phi T+\Phi u_2^0)+\int_\Sigma(\frac{\partial u_1}{\partial \boldsymbol{n}}-\frac{\partial u_2}{\partial \boldsymbol{n}}+\frac{\partial u_2}{\partial \boldsymbol{n}}-\frac{\partial u_2^0}{\partial \boldsymbol{n}}+\frac{\partial u_1^0}{\partial \boldsymbol{n}}-\frac{\partial u_1}{\partial \boldsymbol{n}})g \\ &\quad+\int_{\Gamma_u}\Big[(\eta-\frac{\partial u_2}{\partial \boldsymbol{n}})(u_1-\tau)+(\eta\tau-\frac{\partial u_2}{\partial \boldsymbol{n}}u_1)-\eta u_1^0-\tau\frac{\partial u_2^0}{\partial \boldsymbol{n}}\Big] \\ &= \int_\Omega f(u_2^0-u_1^0)+\int_{\Gamma_m}(\frac{\partial u_1^0}{\partial \boldsymbol{n}}T-2\Phi T+\Phi u_2^0)+\int_\Sigma(\frac{\partial u_1^0}{\partial \boldsymbol{n}}-\frac{\partial u_2^0}{\partial \boldsymbol{n}})g \\ &\quad+\int_{\Gamma_u}\Big[\eta(u_1-u_1^0)+\tau(\frac{\partial u_2}{\partial \boldsymbol{n}}-\frac{\partial u_2^0}{\partial \boldsymbol{n}})-2\frac{\partial u_2}{\partial \boldsymbol{n}}u_1\Big] \end{aligned}$$

Let $C_0=\int_\Omega f(u_2^0-u_1^0)+\int_{\Gamma_m}(\frac{\partial u_1^0}{\partial \boldsymbol{n}}T-2\Phi T+\Phi u_2^0)+\int_\Sigma(\frac{\partial u_1^0}{\partial \boldsymbol{n}}-\frac{\partial u_2^0}{\partial \boldsymbol{n}})g-2\int_{\Gamma_u}\frac{\partial u_2^0}{\partial \boldsymbol{n}}u_1^0$, and using the fact that $u_1=u_1^*+u_1^0$ and $u_2=u_2^*+u_2^0$, we obtain

$$\begin{aligned} E(\eta,\tau) &= \int_\Omega f(u_2^0-u_1^0)+\int_{\Gamma_m}(\frac{\partial u_1^0}{\partial \boldsymbol{n}}T-2\Phi T+\Phi u_2^0)+\int_\Sigma(\frac{\partial u_1^0}{\partial \boldsymbol{n}}-\frac{\partial u_2^0}{\partial \boldsymbol{n}})g \\ &\quad+\int_{\Gamma_u}\Big[\eta u_1^*+\tau\frac{\partial u_2^*}{\partial \boldsymbol{n}}-2(\frac{\partial u_2^*}{\partial \boldsymbol{n}}+\frac{\partial u_2^0}{\partial \boldsymbol{n}})(u_1^*+u_1^0)\Big] \\ &= \int_\Omega f(u_2^0-u_1^0)+\int_{\Gamma_m}(\frac{\partial u_1^0}{\partial \boldsymbol{n}}T-2\Phi T+\Phi u_2^0)+\int_\Sigma(\frac{\partial u_1^0}{\partial \boldsymbol{n}}-\frac{\partial u_2^0}{\partial \boldsymbol{n}})g-2\int_{\Gamma_u}\frac{\partial u_2^0}{\partial \boldsymbol{n}}u_1^0 \\ &\quad-2\int_{\Gamma_u}(\frac{\partial u_2^*}{\partial \boldsymbol{n}}u_1^0+\frac{\partial u_2^0}{\partial \boldsymbol{n}}u_1^*)+\int_{\Gamma_u}\Big[\eta u_1^*+\tau\frac{\partial u_2^*}{\partial \boldsymbol{n}}-2\frac{\partial u_2^*}{\partial \boldsymbol{n}}u_1^*\Big] \\ &= C_0-2\int_{\Gamma_u}(\frac{\partial u_2^*}{\partial \boldsymbol{n}}u_1^0+\frac{\partial u_2^0}{\partial \boldsymbol{n}}u_1^*)+\int_{\Gamma_u}\Big[\eta u_1^*+\tau\frac{\partial u_2^*}{\partial \boldsymbol{n}}-2\frac{\partial u_2^*}{\partial \boldsymbol{n}}u_1^*\Big] \\ &= C_0-2\int_{\Gamma_u}(\frac{\partial u_2^*}{\partial \boldsymbol{n}}v_2^0+\frac{\partial v_1^0}{\partial \boldsymbol{n}}u_1^*)+\int_{\Gamma_u}\Big[(\eta-\frac{\partial u_2^*}{\partial \boldsymbol{n}})u_1^*+(\tau-u_1^*)\frac{\partial u_2^*}{\partial \boldsymbol{n}}\Big] \\ &= C_0-2\int_{\Gamma_u}(\frac{\partial u_2^*}{\partial \boldsymbol{n}}v_2^0+\frac{\partial v_1^0}{\partial \boldsymbol{n}}u_1^*)-\int_{\Gamma_u}\Big[\frac{\partial v_1^*}{\partial \boldsymbol{n}}u_1^*+v_2^*\frac{\partial u_2^*}{\partial \boldsymbol{n}}\Big] \end{aligned}$$

Then by applying Green formula to terms $\frac{\partial u_2^*}{\partial \boldsymbol{n}}v_2^0$, $\frac{\partial v_1^0}{\partial \boldsymbol{n}}u_1^*$, $\frac{\partial v_1^*}{\partial \boldsymbol{n}}u_1^*$ and $v_2^*\frac{\partial u_2^*}{\partial \boldsymbol{n}}$,

$$\int_{\Gamma_u}\frac{\partial u_2^*}{\partial \boldsymbol{n}}v_2^0=\int_\Omega\Delta u_2^*v_2^0+\int_\Omega\nabla u_2^*\nabla v_2^0=\int_\Omega u_2^*v_2^0-\int_\Omega u_2^*\Delta v_2^0+\int_{\Gamma_u}\frac{\partial v_2^0}{\partial \boldsymbol{n}}u_2^*=\int_{\Gamma_u}\frac{\partial v_2^0}{\partial \boldsymbol{n}}\tau$$

$$\int_{\Gamma_u}\frac{\partial v_1^0}{\partial \boldsymbol{n}}u_1^*=\int_\Omega\Delta v_1^0u_1^*+\int_\Omega\nabla v_1^0\nabla u_1^*=\int_\Omega v_1^0u_1^*-\int_\Omega v_1^0\Delta u_1^*+\int_{\Gamma_u}\frac{\partial u_1^*}{\partial \boldsymbol{n}}v_1^0=\int_{\Gamma_u}\eta v_1^0$$

$$\int_{\Gamma_u}\frac{\partial v_1^*}{\partial \boldsymbol{n}}u_1^*=\int_\Omega\Delta v_1^*u_1^*+\int_\Omega\nabla v_1^*\nabla u_1^*=\int_\Omega v_1^*u_1^*-\int_\Omega v_1^*\Delta u_1^*+\int_{\Gamma_u}\frac{\partial u_1^*}{\partial \boldsymbol{n}}v_1^*=\int_{\Gamma_u}\eta v_1^*$$

$$\int_{\Gamma_u}\frac{\partial u_2^*}{\partial \boldsymbol{n}}v_2^*=\int_\Omega\Delta u_2^*v_2^*+\int_\Omega\nabla u_2^*\nabla v_2^*=\int_\Omega u_2^*v_2^*-\int_\Omega u_2^*\Delta v_2^*+\int_{\Gamma_u}\frac{\partial v_2^*}{\partial \boldsymbol{n}}u_2^*=\int_{\Gamma_u}\tau\frac{\partial v_2^*}{\partial \boldsymbol{n}}$$

the final expression of the energy functional becomes

$$E(\eta,\tau)=C_0-2\int_{\Gamma_u}(\eta v_1^0+\tau\frac{\partial v_2^0}{\partial \boldsymbol{n}})-\int_{\Gamma_u}(\eta v_1^*+\tau\frac{\partial v_2^*}{\partial \boldsymbol{n}})=C_0-2b(\eta,\tau)^T+(\eta,\tau)A(\eta,\tau)^T$$

Concerning the symmetry of A, let $(\eta,\tau),(\psi,h)\in H_{00}^{-\frac{1}{2}}(\Gamma_u)\times H_{00}^{\frac{1}{2}}(\Gamma_u)$. It is easy to see that

$$
\begin{aligned}
\left(A(\eta,\tau)^T,(\psi,h)^T\right) &= \int_\Omega (\nabla u_1^*(\eta,\tau)-\nabla u_2^*(\eta,\tau))(\nabla u_1^*(\psi,h)-\nabla u_2^*(\psi,h)) \\
&\quad + \int_\Omega (u_1^*(\eta,\tau)-u_2^*(\eta,\tau))(u_1^*(\psi,h)-u_2^*(\psi,h)) \\
&= \int_\Omega (\nabla u_1^*(\psi,h)-\nabla u_2^*(\psi,h))(\nabla u_1^*(\eta,\tau)-\nabla u_2^*(\eta,\tau)) \\
&\quad + \int_\Omega (u_1^*(\psi,h)-u_2^*(\psi,h))(u_1^*(\eta,\tau)-u_2^*(\eta,\tau)) \\
&= \left((\eta,\tau)^T,A(\psi,h)^T\right)
\end{aligned}
$$

Now, in order to prove that A is a positive-definite operator, consider $(\eta,\tau)\neq(0,0)$ then

$$
\left(A(\eta,\tau)^T,(\eta,\tau)^T\right) = \int_\Omega (\nabla u_1^*-\nabla u_2^*)^2+\int_\Omega (u_1^*-u_2^*)^2 \geq 0
$$

Suppose that $\left(A(\eta,\tau)^T,(\eta,\tau)^T\right)=0$ then $u_1^*=u_2^*$ which implies that $\left(u_1^*(\eta,\tau)|_{\Gamma_m},\dfrac{\partial u_1^*(\eta,\tau)}{\partial \boldsymbol{n}}|_{\Gamma_m}\right)=(0,0)$ then by using Holmgren's uniqueness theorem, $u_1^*=u_2^*=0$ which is impossible because $\left(u_1^*(\eta,\tau)|_{\Gamma_u},\dfrac{\partial u_2^*(\eta,\tau)}{\partial \boldsymbol{n}}|_{\Gamma_u}\right)\neq(0,0)$. Thus, $\left(A(\eta,\tau),(\eta,\tau)^T\right)>0$ and the proof is completed.

REFERENCES

[1] Addouche M, Bouarroudj N, Jday F, Henry J, Zemzemi N. *Analysis of the ECGI inverse problem solution with respect to the measurement boundary size and the distribution of noise*. Math. Model. Nat. Phenom., EDP Sciences, In press.

[2] Andrieux S, Baranger T.N, Ben Abda A. *Solving Cauchy problems by minimizing an energy-like functional*. Inverse Problems, **22** (2006) 115-133.

[3] Andrieux S, Ben Abda A, Baranger T.N. *Data completion via an energy error functional*. C. R. Mecanique. **333**, No.2(2005) 171-177.

[4] Ben Abda A, Henry J, Jaday F. *Boundary data Completion: The method of boundary value problem factorization*. Inverse Problems. **27**, No.5(2011) 055014.

[5] Ben Abda A, Henry J, Jaday F. *Missing boundary data reconstruction by the factorization method*. C. R. Math. Acad. Sci. Paris Ser. I. **347**(2009) 501-504.

[6] Dautray R, Lions J.L. *Mathematical analysis and numerical methods for science and technology Functional and Variational Methods (2)*, Springer, Berlein, 1988.

[7] Engl H.W, Leitao A. *A mann iterative regularization method for elliptic Cauchy problems*, Numerical Functional Analysis and Optimization, **22**(2001) 861-884.

[8] Hadamard J. *Lectures on Cauchy's Problem in Linear Partial Differential Equations*, London : Oxford University Press, 1923.

[9] Hadamard J. *Lectures on Cauchy's Problem in Linear Partial Differential Equations*, Dover, New York, 1952.

[10] Isakov V. *Inverse Problems for Partial Differential Equations*, Applied Mathematical Sciences Springer-Verlag (third edition), New York, 2017.

[11] Jourhmane M, Nachaoui A. *An alternating method for an inverse Cauchy problem*, Numerical Algorithms, **21**(1999) 247-260.

[12] Kohn R, Vogelius M. *Determining conductivity by boundary measurements: II. Interior results*, Comm. Pure Appl. Math., **38**, No.5(1985) 643-667.

[13] Kozlov V.A, Maz'ya V.G, Fomin D.V. *An iterative method for solving the Cauchy problem for elliptic equation*, Comput. Math. Phys., **31**(1991) 45-52.

[14] Lesnic, D., Elliott, L., Ingham, D. B., 1997. *An iterative boundary element method for solving numerically the Cauchy problem for the Laplace equation*, Engineering Analysis with Boundary Elements. **20**, No.2(1997) 123-133.

[15] Maranzana G, Perry I, Maillet D. *Mini and micro-channels: influence of axial conduction in the wall*, International Journal of Heat and Mass Tranfert, **47**(2004) 3993-4004.

[16] Morini G. *Single-phase convective heat transfer in microchannels: A review of experimental results*. International Journal of Thermal Sciences, **43**, No.7(2004) 631-651.

[17] Rouizi Y, Maillet D, Jannot Y, Perry I. *Inverse problem of fluid temperature estimation inside a flat minichannel starting from temperature measurements over its external walls*, European Congress on Computational Methods in Applied Sciences and Engineering (ECCOMAS), Vienna, Austria, September, 2002.

[18] Tajani C, Abouchabaka J, Abdoun O. *KMF Algorithm for Solving the Cauchy Problem for Helmholtz Equation*, Applied Mathematical Sciences, **6**, No.92 (2006) 4577-4587.